ISSN 1070-3284, Russian Journal of Coordination Chemistry, 2014, Vol. 40, No. 10, pp. 726–739. © Pleiades Publishing, Ltd., 2014.
Original Russian Text © I.V. Smolyaninov, A.I. Poddel'sky, S.A. Smolyaninova, N.T. Berberova, 2014, published in Koordinatsionnaya Khimiya, 2014, Vol. 40, No. 10, pp. 608–622.

Penta- and Hexacoordinate Antimony(V) Compounds with the Tridentate O,N,O-Donor Ligand: Electrochemical Transformations and Antiradical Activity

I. V. Smolyaninov[a, *], A. I. Poddel'sky[b], S. A. Smolyaninova[a], and N. T. Berberova[a]

[a] *Astrakhan State Technical University, ul. Tatishcheva 16, Astrakhan, 414025 Russia*

[b] *Razuvaev Institute of Organometallic Chemistry, Russian Academy of Sciences, ul. Tropinina 49, Nizhnii Novgorod, 603600 Russia*

**e-mail: ivsmolyaninov@gmail.com*

Received January 29, 2014

Abstract—The electrochemical transformations and antiradical activity of penta- and hexacoordinate antimony(V) complexes **I**–**V** containing the tridentate O,N,O-donor ligand, N,N-bis(di-3,5-*tert*-butyl-2-hydroxyphenyl)amine, are studied. The oxidation of hexacoordinate triarylantimony(V) compounds $R_3Sb(Cat\text{-}NH\text{-}Cat)$ (**I**–**III**) leads to the formation of neutral paramagnetic intermediates **Ia**–**IIIa**. Two anodic reversible one-electron stages are observed for pentacoordinate complexes $R'_2Sb(Cat\text{-}N\text{-}Cat)$ (**IV**, **V**). The possibility of the formation of stable paramagnetic species in electrochemical oxidation is a reason for the antiradical activity of the complexes. The study of the reactions of compounds **I**–**V** with the electrogenerated superoxide radical anion, diphenylpicrylhydrazyl radical, peroxy radicals, and hydroperoxides formed by the autooxidation of unsaturated fatty acids (oleic, linoleic) shows that all complexes exhibit a pronounced antiradical activity. The highest effect is observed for compounds **I**, **IV**, and **V** characterized by the prolonged action.

DOI: 10.1134/S1070328414090097

INTRODUCTION

Organometallic compounds of transition and nontransition metals with redox-active ligands are among the most intensely studied objects in the chemistry of coordination and organometallic compounds. In a series of paramagnetic organic ligands in the composition of coordination compounds, phenoxyl, nitroxyl, and *o*-semiquinone radicals are sufficiently studied. Tridentate N,N-bis(di-3,5-*tert*-butyl-2-hydroxyphenyl)amine (CatH-NH-CatH) studied in this work can be assigned to the above listed redox-active ligands. Interest in metal complexes with this ligand is due to a diversity of these properties: a phenomenon of redox isomerism [1, 2], various types of exchange interactions [3, 4], catalytic activity [5, 6], and the participation of atoms or groups in transfer reactions [7–9]. The properties manifested by the compounds are related to the ability of the ligand to enter redox transformations due to its ability to exist in four different redox forms (Cat is the catecholate, SQ represents the iminosemiquinone form, and BQ is the corresponding iminobenzoquinone) (Scheme 1).

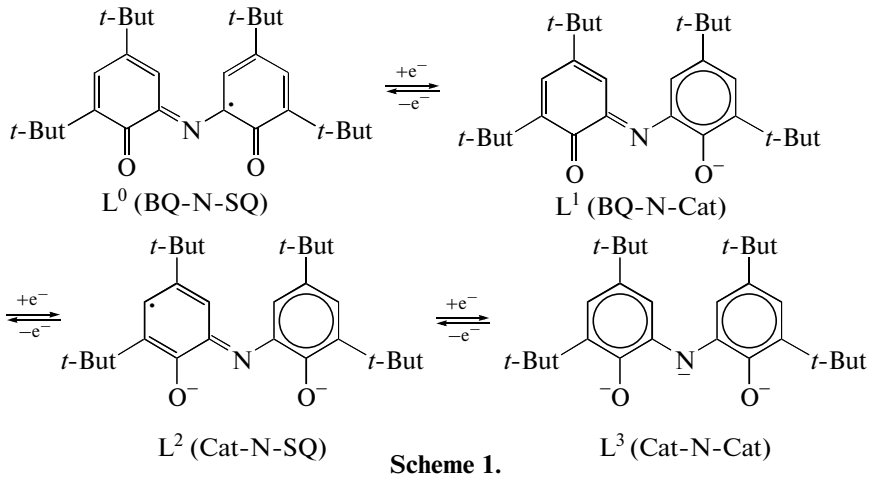

Scheme 1.

There is a wide range of metals for which the complexes containing ligand CatH-NH-CatH were obtained [10–13]. A peak of research activity is presently observed in the chemistry of coordination compounds with this ligand [14–16]. A combination of a redox-active ligand of a similar type with nontransition metals makes it possible to considerably extent their reactive possibilities due to the partial or direct participation of the ligand in a change in the oxidation state of the complex in the course of the reaction. The studies devoted to the antimony(V) complexes with the redox-active ligands, including CatH-NH-CatH, appeared recently [17, 18]. The organometallic compounds containing redox-active fragments were found to exhibit an unusual reactivity: they interact with "small" molecules (O_2, NO, H_2S) [19–24], form "breathing" polymer compositions capable of absorbing oxygen [25], exhibit anticancer, antibacterial, and antiradical activity [26–30], and inhibit in vitro and in vivo lipid peroxidation [31–33].

In this work, we continue the study of the electrochemical transformations and antiradical activity of hexa-R_3Sb(Cat-NH-Cat) (**I–III**) and pentacoordinate R'_2Sb(Cat-N-Cat) (**IV**, **V**) antimony(V) compounds containing the tridentate O,N,O-donor ligand (Scheme 2).

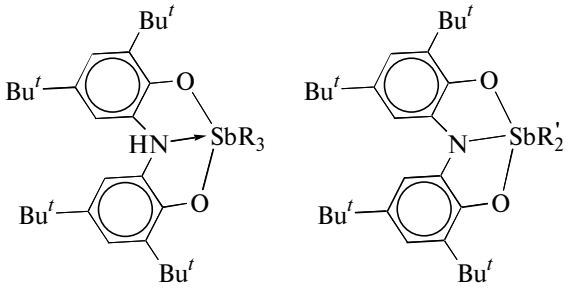

I: R = *n*-Tol; **IV**: R' = Et;
II: R = Ph; **V**: R' = Cyclohex
III: *n*-F-Ph

Scheme 2.

The study of regularities of the electrochemical transformations of organometallic compounds makes it possible to simulate reactions with oxidants and monitor products formed in the reactions. In this work, we studied the electrochemical properties of compounds **I–V**, established the influence of the nature of hydrocarbon groups at the antimony atom on the stability of electrogenerated forms of the complexes, and evaluated their antiradical activity in the reactions with the superoxide radical anion (diphenylpicrylhydrazyl (DPPH) radical) in the inhibition of the oxidation of oleic (*cis*-9-octadecenoic) and linoleic (*cis*,*cis*-9,12-octadecadienoic) acids. Since the redox-active ligand can participate in the oxidative transformations of the complexes, these objects can interact with active forms of oxygen and free radicals and allow one to consider them as potent inhibitors of free radical processes.

EXPERIMENTAL

Compounds **II** and **IV** were synthesized using known procedures [17, 18]. The triarylantimony(V) complexes with the tridentate O,N,O'-ligand (**I** and **III**) were obtained by the reaction of the corresponding triarylstilbene with 4,6-di-*tert*-butyl-N-(2-hydroxo-3,5-di-*tert*-butylphenyl)-*o*-iminobenzoquinone taken in equivalent amounts according to a method similar to that for compound **II** [17]. The complexes are light lilac powders stable in air.

(*n*-Tol)$_3$Sb(Cat-NH-Cat (**I**)

For $C_{49}H_{62}NO_2Sb$			
anal. calcd., %:	C, 71.88;	H, 7.63;	Sb, 14.87.
Found, %:	C, 71.55;	H, 7.51;	Sb, 15.20.

IR, (ν, cm^{-1}): 3306 m, 1597 w, 1564 w, 1481 s, 1412 s, 1387 m, 1362 s, 1298 s, 1279 s, 1265 s, 1239 m, 1229 m, 1202 m, 1189 m, 1168 m, 1128 m, 1089 w, 1072 m, 1067 m, 1060 m, 1021 w, 975 m, 940 w, 914 m, 893 w, 882 m, 861 w, 833 s, 811 m, 797 s, 783 m, 762 w, 749 m, 706 w, 691 w, 677 w, 669 w, 646 w, 596 m, 581 w, 571 m, 527 m, 516 m, 490 s, 442 w, 431 w, 419 m, 405 m.

^{1}H NMR ($CDCl_3$), δ, ppm: 1.21 and 1.30 (both s, 9H each; 2*t*-Bu), 2.23 (s, 6H, 2 CH_3, Sb(*p*-Tol)$_3$), 2.40 (s, 3H, CH_3, Sb(*p*-Tol)$_3$), 5.49 (s, 1H, NH), 6.95 (d, 3*J*(H,H) = 7.8 Hz, 4 *m*-H, *p*-Tol), 7.02 and 7.11 (both d, 4*J*(H,H) = 2.2 Hz, 2H each, C_6H_2), 7.25 (d, 3*J*(H,H) = 7.8 Hz, 4 *o*- and 2 *m*-H, *p*-Tol), 7.90 (d, 3*J*(H,H) = 7.8 Hz, 2 *o*-H, *p*-Tol).

(*p*-F-Ph)$_3$Sb(Cat-NH-Cat) (**III**)

For $C_{46}H_{53}F_3NO_2Sb$			
anal. calcd., %:	C, 66.51;	H, 6.43;	Sb, 14.66.
Found, %:	C, 66.23;	H, 6.27;	Sb, 14.87.

IR, (ν, cm^{-1}): 3308 m, 1638 w, 1606 w, 1582 s, 1412 s, 1389 s, 1362 s, 1300 s, 1278 s, 1266 s, 1230 s, 1161 s, 1127 m, 1090 w, 1069 m, 1058 m, 1021 m, 980 m, 940 w, 914 m, 878 m, 822 s, 782 m, 763 w, 749 m, 724 w, 691 w, 679 w, 668 w, 644 w, 600 m, 525 m, 512 s, 494 w, 476 m, 446 w, 413 s.

^{1}H NMR ($CDCl_3$), δ, ppm: 1.22 and 1.28 (both s, 9H each, 2*t*-Bu), 5.47 (s, 1H, NH), 6.87 (t, 3*J*(H,H) ≈ 3*J*(H,F) = 8.8 Hz, 4 *m*-H, Sb(*p*-F-Ph)^3), 7.06 and 7.15 (both d, 4*J*(H,H) = 2.2 Hz, 2H each, C_6H_2), 7.19 (t, 3*J*(H,H) ≈ 3*J*(H,F) = 8.8 Hz, 2 *m*-H, Sb(*p*-F-Ph)$_3$), 7.31 (dd, 3*J*(H,H) = 8.2 Hz, 3*J*(H,F) = 6.1 Hz, 4 *o*-H, Sb(*p*-F-Ph)$_3$), 7.97 (dd, 3*J*(H,H) = 8.2 Hz, 3*J*(H,F) = 6.1 Hz, 2 *o*-H, Sb(*p*-F-Ph)$_3$).

Synthesis of complex V. A solution of tricyclohexylantimony (0.5 mmol) in toluene (20 mL) was added dropwise to a solution of 4,6-di-*tert*-butyl-N-(3,5-di-*tert*-butyl-2-hydroxyphenyl)-*o*-iminobenzoquinone (IBQ-AP)H (0.5 mmol) in toluene (25 mL) at room temperature. After the violet color of the solution disappeared, toluene was replaced by hexane. A yellow precipitate formed after cooling of the solution was filtered off and recrystallized from the new portion of hexane.

$(Cyclohex)_2Sb(Cat\text{-}N\text{-}Cat)$ (**V**)

For $C_{40}H_{62}NO_2Sb$			
anal. calcd., %:	C, 67.60;	H, 8.79;	Sb, 17.13.
Found, %:	C, 67.39;	H, 8.66;	S, 17.40.

IR, (ν, cm^{-1}): 1588 w, 1567 m, 1478 m, 1443 s, 1418 m, 1354 m, 1347 m, 1321 m, 1279 m, 1259 m, 1241 s, 1213 m, 1202 m, 1173 m, 1136 m, 1097 w, 1050 m, 1013 m, 991 m, 955 m, 912 w, 858 m, 841 m, 822 w, 753 w, 739 w, 676 w, 640 m, 547 m, 531 m, 502 m.

^1H NMR ($CDCl_3$), δ, ppm: 1.2–1.5 (m, 4H, CH_2, cyclohexyl), 1.37 and 1.46 (both s, 18 H each; 2*t*-Bu), 1.55–2.20 (m, 16H, CH_2, cyclohexyl), 2.81 (tt, $3J(H,H) = 11.8$ Hz, $3J(H,H) = 3.6$ Hz, 2H, CH, cyclohexyl), 6.81 (d, $4J(H,H) = 2.1$ Hz, 2H, C_6H_2), 7.76 (d, $4J(H,H) = 2.1$ Hz, 2H, C_6H_2).

^1H, ^{13}C NMR spectra were recorded on a Bruker AVANCE DPX-200 spectrometer using tetramethylsilane as an internal standard and $CDCl_3$ as a solvent. IR spectra were recorded on an FSM 1201 FT-IR spectrometer in Nujol. Experiments on syntheses of the complexes were carried out in evacuated ampules in the absence of oxygen. Absorption spectra were detected on an SF-103 spectrophotomer (in the range from 220 to 1100 nm) at room temperature. EPR spectra were measured on a Bruker EMX spectrometer (working frequency ≈9.5 GHz). Hyperfine coupling (HFC) constants were determined by the simulation of theoretical spectra using the Simfonia program (Bruker). The solvents used were purified and dehydrated according to standard procedures [34].

The following commercial reagents were used without additional purification: DPPH radical (Aldrich), 2,6-di-*tert*-butyl-4-methylphenol (ionol) (Fluka, 99%), $[(C_5H_5)_2Fe]BF_4$ (Aldrich), and oleic (*cis*-9-octadecenoic, 97% Acros Organics) and linoleic (*cis*,*cis*-9,12-octadecadienoic, 99% Acros Organics) acids.

The electrochemical potentials of the studied compounds were measured by cyclic voltammetry (CV) in a three-electrode cell using an IPC-pro potentiostat in dichloromethane under argon. The working electrode was a stationary glassy carbon (GC) electrode with a diameter of 2 mm, and a platinum wire ($S = 18$ mm^2) served as an auxiliary electrode. The reference electrode was an Ag/AgCl/KCl electrode with an electroconducting water-impervious membrane. The concentration of compounds **I–V** was 0.003 mol/L. The number of electrons transferred in the course of the electrode process was estimated relatively to ferrocene used as a standard. The potential sweep rate was 0.2 V/s^{-1}. The supporting electrolyte was 0.1 M Bu_4NClO_4 (99%, Acros). Microelectrolysis of complexes **I**, **II**, and **V** were carried out with a PI-50-1.1 potentiostat on stationary platinum electrodes (plates with a surface area of 30 mm^2) in an undivided three-electrode cell (volume 2 mL) at potentials of 1.3 V (for **I** and **III**) and 0.7 V (for **V**). In both cases, the electrolysis time was 3 h. The conversion of complexes **I**, **III**, and **V** was 84, 75, and 92%, respectively. An Ag/AgCl/KCl electrode with the electroconducting water-impervious membrane was used as a reference electrode. The complex under study ($c = 0.003$ mol/L) was added to the pre-deaerated electrochemical cell containing a solution of a supporting electrolyte (0.1 M *n*-Bu_4NClO_4) in dichloromethane.

The reactions of complexes **I**, **III**, and **V** with the superoxide radical anion were carried out in acetonitrile, and the solution was preliminarily purged with oxygen for 10 min to attain saturation. The superoxide radical anion was generated by the electrochemical reduction of oxygen at a potential of −1.0 V. The oxygen concentration was determined by microcoulometry and was equal to 0.003 mol/L. Microelectrolyses of the complexes (c = 0.003 mol/L) in the presence of oxygen were carried out at a specified potential of −1.0 V.

The antiradical activity of complexes **I–V** in the reactions with the DPPH radical in dichloromethane was determined by an earlier described electrochemical procedure [35] for 1 h. The GC electrode was thoroughly cleaned prior to each measurement. The initial concentration of the DPPH radical (c_0) was 0.5×10^{-3} mol/L, and the mole ratio of the DPPH radical to complex **I–V** was 2 : 1. The reaction mixture was incubated at 298 K for 1 h. At the end of the experiment, the cyclic voltammograms were recorded three times. The average values of the obtained concentrations of the DPPH radical are presented in the work. The change in the DPPH radical concentration was determined from a decrease in the intensity of its cathodic peaks ($E^1_{pc} = 0.86$ V; $E^2_{pc} = 0.27$ V) after the end of the experiment. The concentration of the DPPH radical at the moment of reaction end (c_i) was determined from the calibration dependence ($f(c) = I$), which is rectilinear and passes through the origin (correlation coefficient $r = 0.9945$). The value of antiradical activity (***A***) was calculated by the formula $A = (1 - c_i/c_0) \times 100\%$.

Oleic acid was oxidized in the presence of compounds **I–III** in a temperature-controlled cell (60°C) at an air flow rate of 2–4 mL/min for 5 h. Since oleic acid oxidation proceeds as autooxidation, preliminary air bubbling was carried out for 2 h before the intro-

Table 1. Oxidation potentials of the antimony(V) complexes according to the CV method[a, b]

Compound	E^1_{pa}, V[b]	I_c/I_a	n	E^2_{pa}, V[b]	n[b]	I_c/I_c	E^3_{pa}, V[b]	ΔE, V
(n-Tol)$_3$Sb(Cat-NH-Cat) (I)	1.09		1.5	1.75	1.0			
Ph$_3$Sb(Cat-NH-Cat) (II)	1.13		1.6					
(n-F-Ph)$_3$Sb(Cat-NH-Cat) (III)	1.15		1.5	1.73	1.0			
Et$_2$Sb(Cat-N-Cat) (IV)	0.51[d]	1.0	1.0	0.98[e]	1.0	1.0	1.72	0.47
(Cyclohex)$_2$Sb(Cat-N-Cat) (V)	0.52[d]	0.8	1.0	1.01[e]	<1.0	0.4	1.76	0.49
(n-Tol)$_3$Sb(Cat-N-SQ) (Ia)	–0.30[d]	0.9		0.50[e]		0.6		0.84
Ph$_3$Sb(Cat-N-SQ) (IIa)	–0.27[d]	1.0		0.53[e]		0.8		0.80
(n-F-Ph)$_3$Sb(Cat-N-SQ) (IIIa)	–0.21[d]	0.7		0.66				0.76
Ph$_2$Sn(Cat-NH-SQ)[c]	–0.30[d]	0.9	1.0	0.56[e]	1.0	0.9	1.70	0.83

[a] GC electrode; CH_2Cl_2, $V = 0.2$ V/s, 0.1 M NBu_4ClO_4, $c = 3 \times 10^{-3}$ mol/L, Ar, vs. Ag/AgCl/KCl (saturated).

[b] E^1_{pa}–E^3_{pa} are the values of anodic peak potentials (see text), I_c/I_a is the ratio of the currents of the backward cathodic and direct anodic peaks, n is the number of electrons transferred during the redox process relatively to ferrocene as a standard, and $\Delta E = E^2_{1/2} - E^1_{1/2}$.

[c] Published data [38].

[d] Potential of the half-width of the cathodic process ($E^1_{1/2}$).

[e] Potential of the half-width of the anodic process ($E^2_{1/2}$).

duction of the compounds. The concentration of additives was 1 mmol/L. The activity of the studied compounds in the course of oleic acid oxidation was estimated using a standard method from the amount of formed isomeric hydroperoxides LOOH [36]. The inhibition efficiency (IE) of the autooxidation of oleic acid was determined by the formula IE = $(1 - (1 - c_i/c_0) \times 100\%$, where c_i is the concentration of hydroperoxides in the presence of an additive of the complexes (1 mmol/L), and c_0 is the content of LOOH formed in the control sample within 5 h.

Linoleic acid was oxidized in the presence of compounds **II**, **IV**, and **V** and ionol in a thermostat (30°C) for 144 h. In 24 h, three samples were taken and the concentrations of isomeric hydroperoxides were determined by iodometric titration. The amount of carbonyl compounds was estimated in a test with thiobarbituric acid from the formation of a colored pigment (TBARS), whose concentration was measured spectrophotometrically at 532 nm [37]. The results are presented as average values of three independent experiments.

RESULTS AND DISCUSSION

Electrochemical transformations of complexes I–V. The electrochemical properties of antimony(V) compounds **I**–**III** were studied by the CV method (Table 1). The oxidation of complexes R_3Sb(Cat-NH-Cat) on the GC electrode in dichloromethane is irreversible, and the number of electrons transferred in the first anodic stage exceeds unity (Fig. 1).

The electrochemical activity observed for complexes **I**–**III** can be considered as a change in the

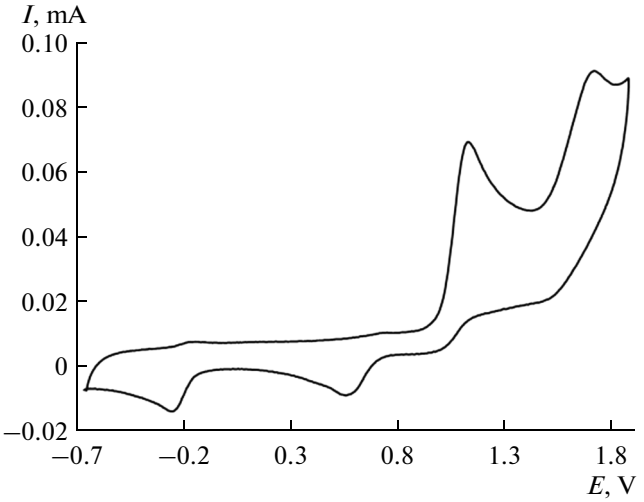

Fig. 1. Cyclic voltammogram of the oxidation of complex **III**.

redox state of the coordinated ligand. The oxidation of the compounds affords unstable radical cation complexes that further undergo deprotonation to form neutral paramagnetic derivatives $R_3Sb(Cat\text{-}N\text{-}SQ)$ (**Ia–IIIa**) (Scheme 3).

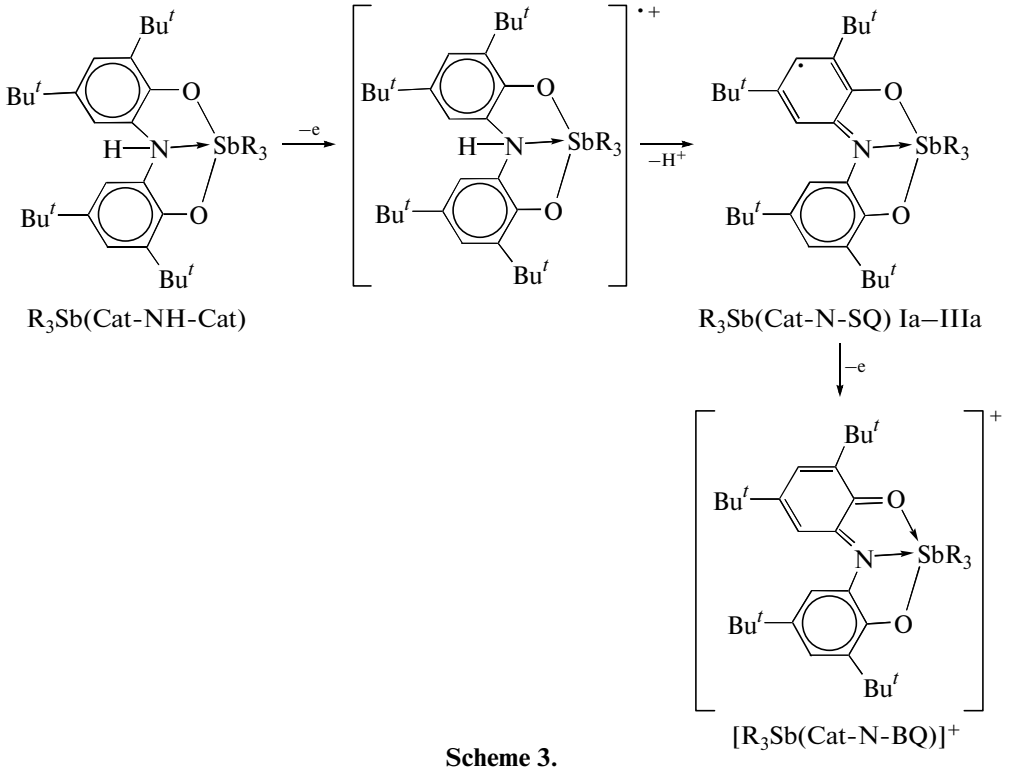

Scheme 3.

The oxidation potentials of paramagnetic complexes **Ia–IIIa** are shifted to the cathodic region compared to initial compounds **I–III**, which leads to their further oxidation. The result of the consecutive ECE stages of the electrode process (E and C are the electrochemical and chemical stages in the solution bulk, respectively) is the generation of a proton and cationic complexes $[R_3Sb(Cat\text{-}N\text{-}BQ)]^+$ in the solution. The formation of the cationic complexes is indicated by the re-reduction peaks of $[R_3Sb(Cat\text{-}N\text{-}BQ)]^+$ detected at the reverse branch of the CV curve (E_{pc1} = 0.48–0.56 V; E_{pc2} = –0.37 to –0.26 V) corresponding to the redox transitions $[R_3Sb(Cat\text{-}N\text{-}BQ)]^+/[R_3Sb(Cat\text{-}N\text{-}SQ)]$ and $[R_3Sb(Cat\text{-}N\text{-}SQ)]/[R_3Sb(Cat\text{-}N\text{-}Cat)]^-$. Generated in the chemical stage H^+ partially protonates the initial compounds, and the species formed are not oxidized in this potential sweep range due to which the number of transferred electrons exceeds unity.

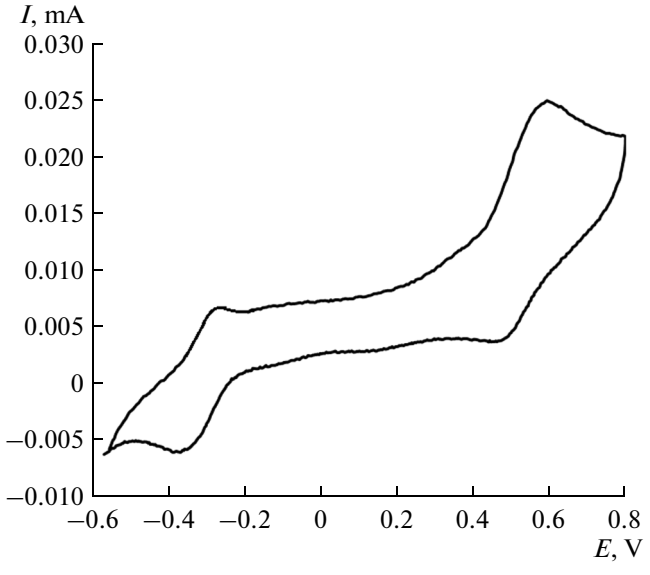

Fig. 2. Cyclic voltammogram of the oxidation of the electrolysis product of complex **I**.

The electrolysis of compounds **I** and **III** in CH_2Cl_2 was carried out at a controlled potential of +1.3 V in order to generate paramagnetic species of complexes **Ia** and **IIIa**. As a result, reversible redox transitions appear in the CV curve (Fig. 2) shifted to the cathodic region (Table 1).

The detected redox processes correspond to a change in the oxidation state of the coordinated π-radical ligand in paramagnetic intermediates **Ia** and **IIIa** formed due to electrolysis (Table 1) (Scheme 4). Similar data were obtained earlier for compound **II** [39].

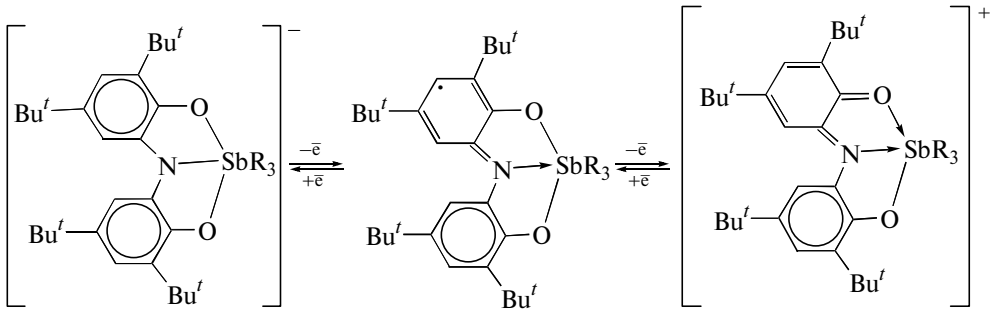

Scheme 4.

Cationic complexes $[R_3Sb(Cat\text{-}N\text{-}BQ)]^+$ and a proton are the oxidation products of compounds **I** and **III**. However, radicals **Ia** and **IIIa** are accumulated in the electrolysis. Their formation is caused by the possibility of parallel redox processes to occur. Gaseous products are evolved at the auxiliary electrode during electrolysis. Complexes **I** and **III** act as proton donors, resulting in hydrogen evolution. The overall anodic process proceeds as a two-electron process, and two molecules of the complexes are reduced on the cathode to form two anions $[R_3Sb(Cat\text{-}N\text{-}Cat)]^-$. The diffusion of the redox transformation products into the solution assumes the possibility of the comproportionation between $[R_3Sb(Cat\text{-}N\text{-}Cat)]^-$ and $[R_3Sb(Cat\text{-}N\text{-}BQ)]^+$ to finally form two radicals of types **Ia** and **IIIa**.

The electrolysis of compounds **I–III** is accompanied by the intense coloration of the solution into violet. The absorption spectra of the electrolysis products (Fig. 3) exhibit the appearance of new absorption bands in the visible spectral range (λ_1 = 388 nm, λ_{sh} = 500–550 nm) and a broadened absorption band in the long-wavelength spectral range (λ_3 = 864 nm). The observed absorption bands correspond to the intramolecular charge transfer in the coordinated ligand Cat-N-SQ [3, 10].

Unlike compound **II**, compounds **I** and **III** exhibit an additional irreversible one-electron process in the anodic region (Fig. 1). As shown above, the ligand can exist in four different redox forms. For compounds **I** and **III**, the second redox transition (E^2_{pa} = 1.74 V) corresponds to the further oxidation of the monocationic complex $[R_3Sb(Cat\text{-}N\text{-}BQ)]^+$ formed due to the ECE processes to the dication containing a neutral paramagnetic form of the ligand (Scheme 5).

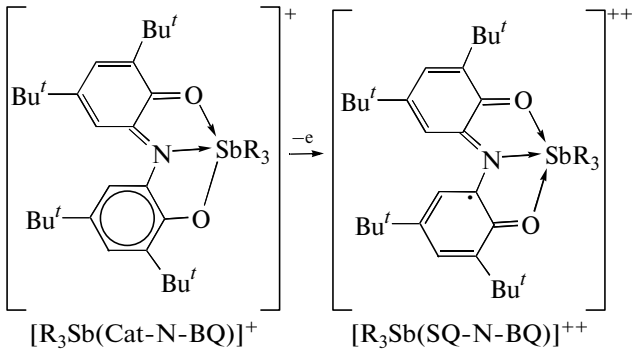

Scheme 5.

The formation of a similar form of the ligand has previously been detected by electrochemical methods in the case of the transition metal complexes [1, 2, 40]. The oxidation potentials (E^2_{pa}) of complexes **I** and **III** are close to those obtained earlier for the tin derivative $Ph_2Sn(Cat\text{-}N\text{-}SQ)$ (E_{pa} = 1.70 V) [38]. However, the electrochemical oxidation of the tin(IV) compound proceeds as a two-electron process, unlike the antimony(V) complexes.

The nature of the substituent in the phenyl ring affects the values of redox potentials of complexes **I–III**. The introduction of a donor hydrocarbon group favors the shift of the oxidation potential to the cathodic region, whereas for complex **III** containing electron-acceptor fluorine atoms, on the contrary, the anodic shift of the oxidation potentials is observed. The substituents in the *para*-position of the phenyl ring exert an effect on both the values of redox potentials of electrogenerated complexes **Ia–IIIa** and stability of the oxidized/reduced forms of the complexes (Table 1). The monocationic and monoanionic forms of **Ia–IIIa** have different stabilities: the redox forms of complex **IIa** is most stable, and the introduction of the electron-acceptor fluorine atom results in the irreversibility of the oxidation of the monocationic form of compound **IIIa**.

$E_{1/2}$ is thermodynamic value for the reversible one-electron redox transitions that makes it possible to estimate the energy of the molecular orbital on which electronic changes occur in the course of the reaction. The values of difference ΔE obtained for the studied complexes allow one to estimate the size of the energy gap HOMO–LUMO. On going from compound **Ia** to **IIIa**, the values of ΔE decrease, indicating that the frontier redox orbitals are brought together. For the pentacoordinate compounds, this parameter decreases to 0.47 and 0.49 V. The values of ΔE for complexes **Ia–IIIa, IV**, and **V** indicate a broad charge and spin delocalization in the paramagnetic species generated under the electrochemical conditions.

As shown for complex **IV** [39], the electrochemical oxidation of compound **V** proceeds similarly in three consecutive stages: the first and second anodic processes have a reversible one-electron character and correspond to the formation of paramagnetic radical cation $[R'_2Sb(Cat\text{-}N\text{-}SQ)]^+$ and dicationic $[R'_2Sb(Cat\text{-}N\text{-}BQ]^{++}$) complexes (Scheme 6).

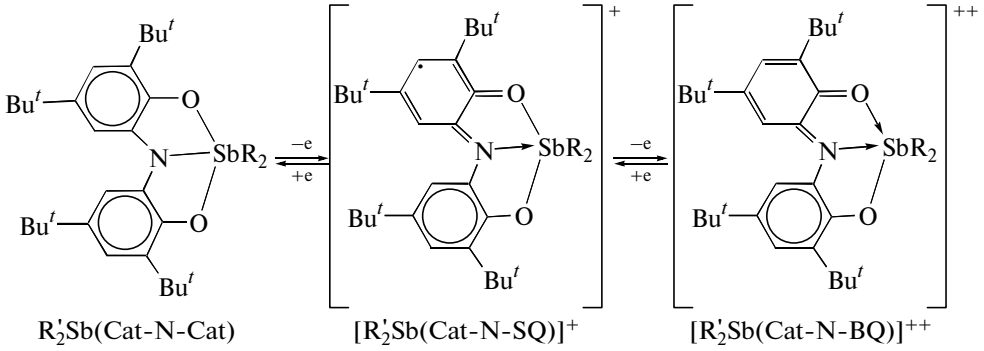

Scheme 6.

The oxidation potentials (E^3_{pa}) of compounds **IV** and **V** and (E^2_{pa}) of compounds **I** and **III** are close and correspond to the formation of a neutral iminobenzosemiquinone form of the ligand (BQ-N-SQ). This anodic redox process is irreversible and results in the decoordination of the ligand and decomposition of the complexes.

The reversibility coefficients (I_c/I_a) (Table 1) indicate that the monocationic forms of complexes **IV** and **V** ($[R'_2Sb(Cat\text{-}N\text{-}SQ)]^+$) formed in oxidation are fairly stable in the experimental time scale. This made it possible to generate radical cation complex $[(Cyclohex)_2Sb(Cat\text{-}N\text{-}SQ)]^+$ in electrolysis at a controlled potential of 0.8 V. The results obtained for the electrolysis of complex **V** are similar to those described earlier for complex **IV**: at the end of electrolysis, the shape of the CV curve remains unchanged and the solution turns intense violet [36]. The absorption bands corresponding to the formation of cationic complex $[(Cyclohex)_2Sb(Cat\text{-}N\text{-}SQ)]^+$ are observed in the visible spectral range (λ_1 = 386 nm, λ_{sh} = 554 nm, λ_3 = 962 nm). Unlike electrogenerated hexacoordinate compounds **Ia–IIIa**, the oxidized forms of complexes **IV** and **V** exhibit the shift of the absorption maximum λ_3 to the near-IR spectral region possibly caused by an increase in the contribution of the orbital of the metal to the molecular orbital containing a lone electron.

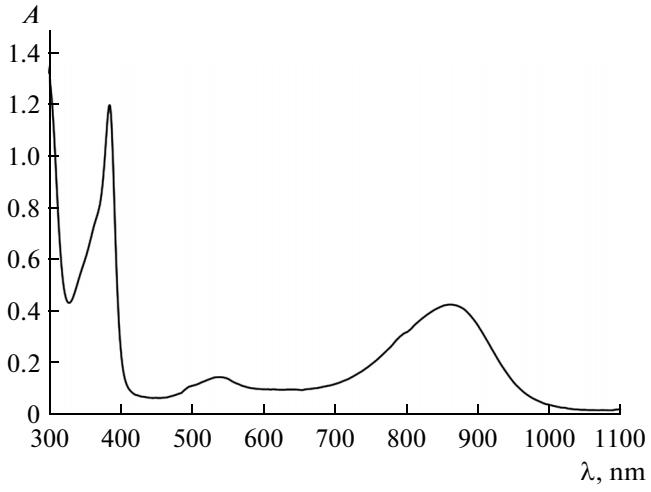

Fig. 3. Absorption spectra of complex **III** in CH_2Cl_2 after 1 h of electrolysis at a potential of 1.30 V (293 K, argon).

The obtained electrochemical data suggest that complexes **I–V** are characterized by fairly low anodic potentials. The easier the oxidation, the higher the probability of the interaction with active radicals. The studied complexes can undergo both hydrogen (**I–III**) and electron (**IV**, **V**) abstraction entering chain termination reactions and forming stable paramagnetic intermediates. Therefore, these objects can be considered as efficient radicals traps.

Antiradical activity. Various methods are presently used for the evaluation of the antioxidant activity of the compounds. One of the known methods is the

ORAC method, being the measurement of the ability to absorb oxygen-containing radicals. The photometric method (fluorimetry) is often used to evaluate the antioxidant activity of various biologically active substances and artificial antioxidants. However, the electrochemical methods based on the generation of a superoxide radical anion in the model system also find use [41–45]. In the present study, we did not aimed at quantitatively estimating the antioxidant capacity of the studied objects. It was necessary to determine (at the qualitative level) the possibility of the interaction of compounds **I–V** with the superoxide radical anion, being one of the active forms of oxygen indirectly involved in the development of the oxidative stress [46]. The reactions of complexes **I–V** with the electrogenerated superoxide radical anion (in situ) were studied. The reactions were carried out in acetonitrile because of the better reproducibility of the CV curves of the superoxide radical anion and its sufficiently long lifetime [47–49]. The electrochemical reduction of oxygen is a one-electron reversible process (E_{pc} = –0.90 V) (Fig. 4, curve *1*). The studied compounds exhibit no electrochemical activity in the potential sweep range (from +0.70 to –1.20 V). The introduction of complexes **I** and **III** into an aerated acetonitrile solution changes the shape of the CV curves (Fig. 4, curve *2*) similarly to that described previously for compound **II** [39]: the reduction of oxygen proceeds as an irreversible process with the appearance of peaks of the chemical reaction products on the reverse anodic branch (0.25 and 0.60 V), and an increase in the number of cycles leads to the appearance of an additional reversible process ($E_{1/2}$ = –0.11 V) (Fig. 4, curve *2*).

The electrolysis of aerated solutions of complexes **I** and **III** at the potential of oxygen reduction (–1.1 V) results in the coloration of the solutions. The absorption spectra of the reaction products are identical to those indicated above for electrogenerated complexes **Ia** and **IIIa**. After electrolysis, the CV curves

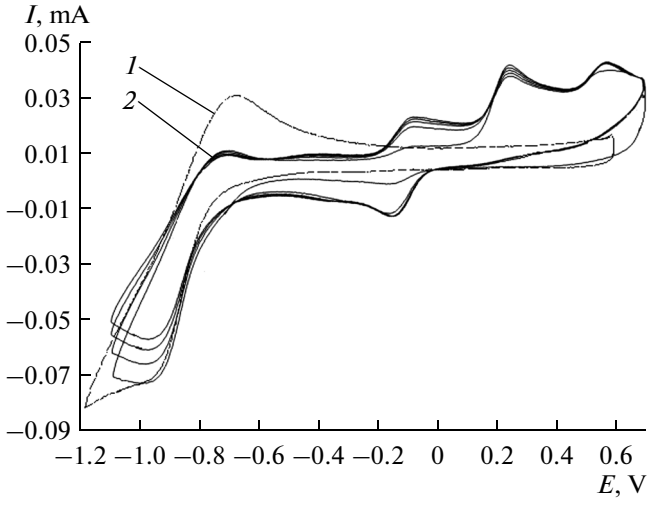

Fig. 4. Cyclic voltammogram of the reduction (CH_3CN) of (*1*) O_2 and (*2*) O_2 in the presence of complex **III** (4 cycles).

exhibit a reversible cathodic process ($E_{1/2}$ = –0.20 (**I**), –0.11 V (**III**)) shifted to the anodic region compared to the data obtained in CH_2Cl_2 and a quasi-reversible anodic process (E_{pa} = 0.50 (**I**), 0.57 V (**III**)). The electrochemical and spectral data are consistent with those obtained earlier for compound **II** and indicate the formation of complexes of the **Ia** and **IIIa** types.

It is known that in acetonitrile and dimethylformamide $O_2^{-\bullet}$ exhibits the basic properties [49, 50]. In the presence of proton donors, the oxidation involving the superoxide radical anion proceeds through the consecutive deprotonation of the substrate followed by the oxidation of the monoanion with the peroxyl radical. Evidently, deprotonation is also the primary stage in the reaction of the superoxide radical anion with complexes **I–III** (Scheme 7).

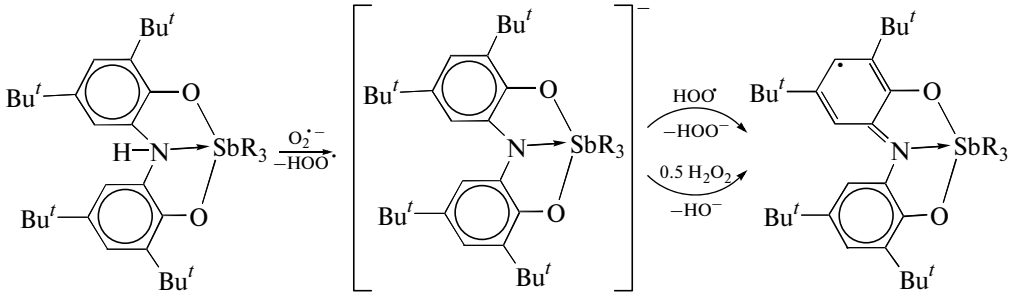

Scheme 7.

Monoanionic complexes $[R_3Sb(Cat\text{-}N\text{-}Cat)]^-$ are subjected to the oxidation by the hydroperoxyl radical or the product of its disproportionation (H_2O_2) to form (in both cases) neutral paramagnetic derivatives **Ia–IIIa**.

The introduction of compounds **IV** and **V** into an aerated solution also changes the shape of the CV curves (Fig. 5). The reduction of oxygen becomes irreversible in the voltammogram, and the anodic peaks of the chemical reaction products on the reverse branch.

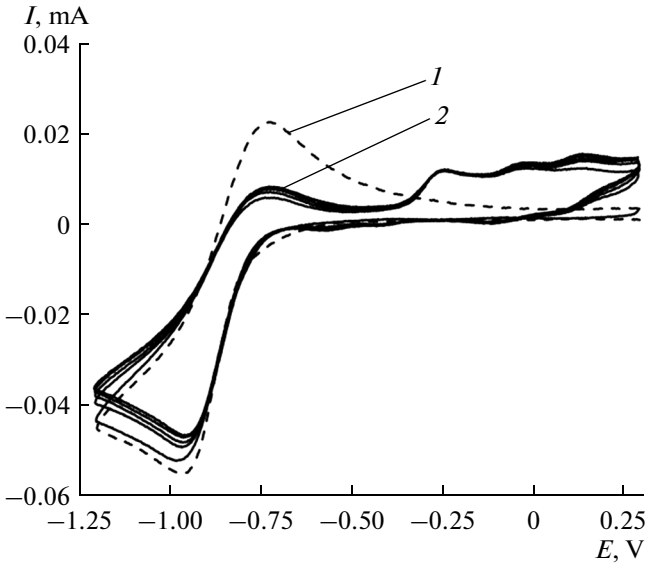

Fig. 5. Cyclic voltammogram of the reduction (CH_3CN) of (*1*) O_2 and (*2*) O_2 in the presence of complex **V** (5 cycles).

The detected changes indicate that these complexes interact with the superoxide radical anion. The electrolysis at a controlled potential in the presence of the pentacoordinate antimony(V) compounds results in the appearance of the solution color characteristic of monocationic complexes $[\mathbf{IV}]^+$ and $[\mathbf{V}]^+$. The absorption spectra of the solutions after electrolysis contain the absorption bands of the monocationic forms of the complexes and an additional band at 465 nm. The shape of the CV curves after electrolysis also differs from the initial shape. The observed changes indicate the partial destruction of the complex that obviously occurs due to the decoordination of the oxidized form of the ligand.

The mechanism proposed for the reactions of the superoxide radical anion with compounds **IV** and **V** differs from that described above for the hexacoordinate compounds, because there is no proton source in this case. Nevertheless, the antimony(V) atom in the pentacoordinate compounds has a vacant molecular orbital that can be presented for the superoxide radical anion being a nucleophilic agent. It was shown earlier when describing the mechanism of molecular oxygen fixation that one of the stages of the process is the oxidation of the redox-active ligand with molecular oxygen and the coordination of $O_2^{-\bullet}$ to the antimony atom [19]. Our preliminary studies of complexes **IV** and **V** with different nucleophilic agents confirm the formation of the neutral and negatively charged hexacoordinate complexes. Due to this, the assumed reaction mechanism at the primary stage includes the coordination of the reduced form of oxygen to the antimony atom followed by the oxidation of the redox-active ligand to the Cat-N-SQ form. The intermediate formed is lowly stable, which results in a side reaction accompanied by the partial decoordination of the ligand.

The reaction of antioxidants with the DPPH radical is one of the known methods for the determination of the antiradical activity [51]. The reaction of the stable DPPH radical with a neutral molecule leads to hydrogen atom abstraction to form the corresponding substituted hydrazine and the radical antioxidant species. The changes that occurs during the reaction are detected by spectrophotometry from a decrease in the absorption band intensity of the DPPH radical in the range from 512 to 527 nm, depending from the solvent used [52–54]. We have previously showed that the triphenylantimony(V) derivatives exhibit a high antiradical activity in this reaction [29, 30]. However, it seems impossible to use spectrophotometry for the determination of the antiradical activity of compounds **I–V** because of the formation of the colored complexes, whose absorption bands in the visible spectral range are similar to those of the DPPH radical.

To estimate the antiradical activity, we used the earlier described electrochemical procedure [35]. The reactions of complexes **I–V** with the DPPH radical were studied by the CV method. The introduction of complexes **I–V** into a solution of the DPPH radical results in a gradual decrease in the intensity of peaks of two one-electron redox transitions corresponding to the oxidized ($E^1_{1/2}$ = 0.90 V) and reduced ($E^2_{1/2}$ = 0.26 V) forms of the DPPH radical. The possibility of the reactions of the complexes with the DPPH radical assumes that these compounds can act as efficient radical scavengers. The reactions of compounds **I–III** with the DPPH radical decrease the concentration of the latter and also lead to the appearance in the voltammograms of reversible redox processes (–0.20... –0.30 and +0.50...+0.62 V) corresponding to the formation of paramagnetic products **Ia–IIIa** (Scheme 8).

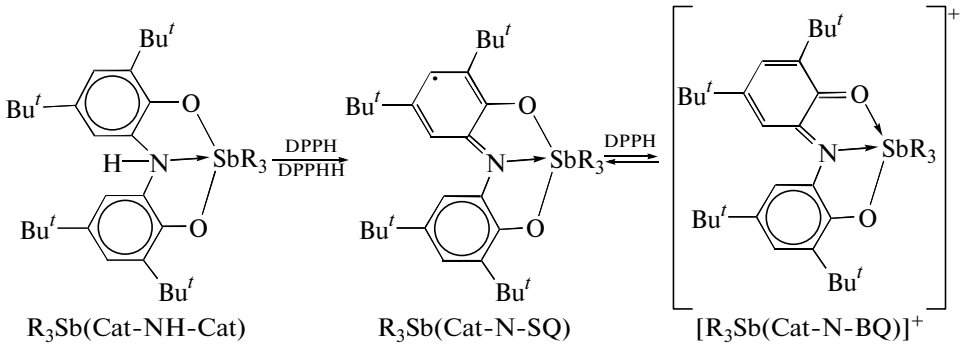

Scheme 8.

The antiradical activity was determined 1 h after the reaction beginning using the formula: $A = (1 - c_i/c_0) \times 100\%$ (Table 2). The obtained values of antiradical activity show that compounds **I–III** can transform only one molecule of the DPPH molecule. The equilibrium of the reaction between two stable radical species (DPPH radical and oxidized forms **Ia–IIIa**) is shifted to the left.

Complexes **IV** and **V** with the oxidation potentials shifted to the cathodic region compared to those of compounds **I–III** exhibit somewhat higher antiradical activity (Table 2). For all compounds studied, the values of A exceed the parameters of ionol obtained earlier by a similar method [55]. Pentacoordinate antimony(V) complexes **IV** and **V** exhibit the antiradical activity compared to that of the compounds containing several phenol fragments [55].

The reactions of compounds **IV** and **V** with the DPPH radical and superoxide radical anions are more complicated in nature. The reactions of complex **V** with the DPPH radical and one-electron oxidant, ferricinium tetrafluoroborate ([Fc]BF_4), were studied by the EPR method. The intensity of the signal from the DPPH radical decreased without the appearance of a spectrum of another paramagnetic species upon the addition of complex **V** to a solution of the DPPH radical. A similar behavior was observed earlier for triphenylantimony(V) *o*-amidophenolate [29]. The absence of signals from the oxidized form of the complex is possibly due to the secondary transformations of the O,N,O-donor ligand (intramolecular cyclization) or formation of adducts with the reduced form of the DPPH radical, which was earlier observed for substituted aromatic amines [54].

The reaction of [Fc]BF_4 with compound **V** affords cationic complex $[(Cyclohex)_2Sb(Cat\text{-}N\text{-}SQ)]^+$ ($[V]^+[BF_4]^-$), whose EPR spectrum has $g_i = 2.0012$ (Fig. 6). The hyperfine structure of the spectrum is caused by the interaction of a lone electron with the magnetic cores of antimony (^{121}Sb, $I = 5/2$, 57.25%, $g_N = 1.34550$; ^{123}Sb, $I = 7/2$, 42.75%, $g_N = 0.72876$) and the magnetic cores of the paramagnetic ligand coordinated through the tridentate mode (by two pairs of protons in positions 3 and 5 of each of two six-membered rings and by one nitrogen atom). The values of HFC constants on the magnetic isotopes of the complex and earlier studied related complexes are shown in Table 3. It should be mentioned that the EPR spectra exhibit only the splitting on the magnetic cores of antimony and the constants on the magnetic cores of the ligands are nearly indiscernible due to a large width of the individual line. However, the computer simulation of the spectrum makes it possible to reproduce the experimentally observed pattern with allowance for these HFC constants only.

The values of HFC constants with the magnetic cores of the paramagnetic O,N,O-donor ligand are similar to those in the EPR spectra of the earlier studied nontransition metal complexes [38, 57, 58]. Unlike the previously studied monocationic triphenylantimony(V) complex with the *o*-iminobenzosemiquinone ligand $[(AP\text{-}ISQ)SbPh_3]^+$ and the neutral hexacoordinate triphenylantimony(V) complex $Ph_3Sb(Cat\text{-}N\text{-}SQ)$, the HFC constants for pentacoordinate ionic complexes $[V]^+[BF_4]^-$ and $[IV]^+[BF_4]^-$ are high. A similar increase in the HFC constants is observed when the coordination number of the central metal atom decreases. In addition, these antimony

Table 2. Antiradical activity (A) of compounds **I–V** in the test with the DPPH radical during oleic acid autooxidation[a]

Compound	A, %	IE, %[b]
$(n\text{-Tol})_3Sb(Cat\text{-}NH\text{-}Cat)$	48.5	87.7
$Ph_3Sb(Cat\text{-}NH\text{-}Cat)$	45.4	82.2
$(n\text{-F-Ph})_3Sb(Cat\text{-}NH\text{-}Cat)$	48.2	85.2
$Et_2Sb(Cat\text{-}N\text{-}Cat)$	60.6	84.0
$(Cyclohex)_2Sb(Cat\text{-}N\text{-}Cat)$	62.0	87.3
2,6-di-*tert*-butyl-4-methylphenol	25.4[c]	65.4

[a] The concentration of the DPPH radical is 0.5×10^{-3} mol/L, and the ratio of concentrations of the DPPH radical to complex **I–V** was 2 : 1. Reaction time 60 min, GC electrode, CH_2Cl_2, GC anode, Ag/AgCl/KCl, 0.1 M NBu_4ClO_4.

[b] IE is the indicator of inhibition efficiency of oleic acid autooxidation.

[c] Published results [55].

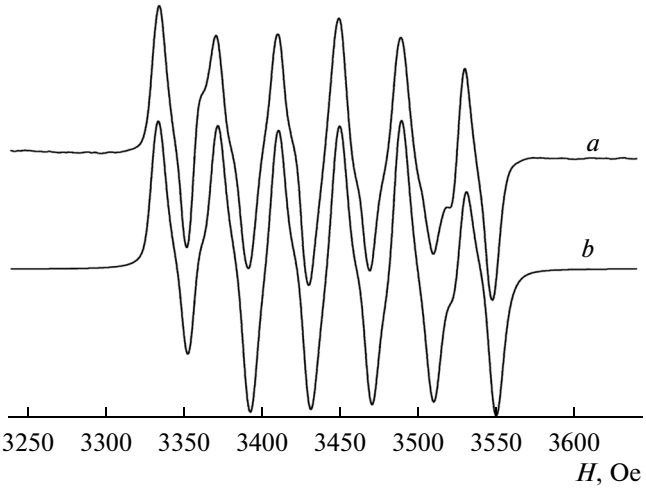

Fig. 6. EPR spectra of paramagnetic complex $[\mathbf{V}]^+[BF_4]^-$: (*a*) experimental (toluene, 293 K and (*b*) computer simulation (WINEPR SimFonia 1.26).

compounds can exhibit somewhat higher shift of the electron density from the ligand to metal than that in neutral Ph_3Sb(Cat-N-SQ).

We studied the antiradical activity of compounds **I–V** toward peroxyl radicals (LOO$^\bullet$) and hydroperoxides (LOOH) formed due to the autooxidation of unsaturated fatty acids (oleic (*cis*-9-octadecenoic (LH)) (60°C) and linoleic (*cis*,*cis*-9,12-octadecadienoic (L'H)) (30°C) acids) as a model reaction of the peroxide oxidation of lipids in cell membranes. The influence of compounds **I–V** on the autooxidation of oleic acid was studied. The kinetic curves of LOOH accumulation are similar for all complexes, and the data for compounds **I**, **II**, and **V** are shown in Fig. 7. The pentacoordinate antimony(V) compounds exhibit somewhat higher inhibiting activity in oleic acid oxidation than the hexacoordinate compounds (Fig. 7).

In the presence of the studied compounds, the concentration of hydroperoxides for the first 2 h steadily decreases compared to the parameters of the control experiment. Then for all compounds the LOOH concentration remains almost unchanged, which corresponds to the induction period. A violet color of the solutions appears in the course of the reaction (1.5 h). The detected absorption spectrum contained bands corresponding to the formation of paramagnetic intermediates. The intensity of the absorption band maxima increases with time. Comparative data on the efficiency of inhibition of the oxidation of oleic acid at 60°C within 5 h in the presence of complexes **I–V** are shown in Table 2. The efficiency of inhibition for compounds **I–V** was found to exceed the data for the known phenol antioxidant ionol.

Complex **I** exhibits the highest activity among the hexacoordinate compounds. The inhibiting influence of compounds **I–V** on the autooxidation of oleic acid is due to the formation of stable paramagnetic intermediates during the reaction with active LOO radicals. In the case of compounds **I–III**, products **Ia–IIIa** are formed (Scheme 9).

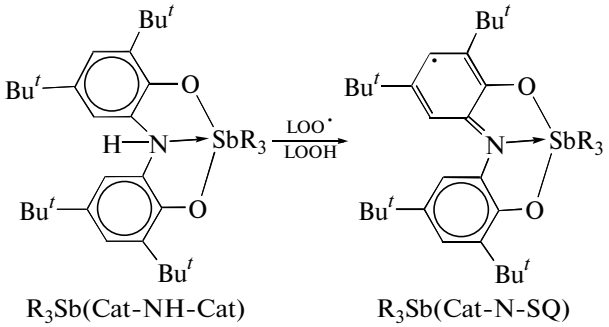

Scheme 9.

The primary decrease in the LOOH concentration indicates that the studied compounds can be considered as inhibitors of the chain radical process and also as destructors of hydroperoxides.

Leader compounds (**I**, **IV**, **V**) that exhibit the highest inhibiting activity can be distinguished in a series of the studied complexes. These compounds were chosen for an experiment with linoleic acid. Hydroperoxides of unsaturated fatty acids are unstable compounds decomposing to form toxic products: malonic dialdehyde and 4-hydroxynonenal. Due to this, the forma-

Table 3. EPR spectral parameters of metal complexes R_nSb(Cat-N-SQ) (toluene, 298 K)

Compound	g_i	A_i(2H), Oe	A_i(2H), Oe	$A_i(^{14}N)$, Oe	A_i(M), Oe	Literature
$[(Cyclohex)_2Sb(Cat\text{-}N\text{-}SQ)]^+[BF_4]^-$	2.0012	1.7	3.5	6.8	39.0/21.14 (^{121}Sb/^{123}Sb)	
$[Et_2Sb(Cat\text{-}N\text{-}SQ)]^+[BF_4]^-$	2.0032	1.7	3.2	6.6	33.6/18.2 (^{121}Sb/^{123}Sb)	[39]
$[(AP\text{-}ISQ)SbPh_3]^+[BF_4]^-$[a]	2.0039	~1.5	~3.1	~7.1	~12.2/6.6 (^{121}Sb/^{123}Sb)	[56]
$[Ph_3Sb(Cat\text{-}N\text{-}SQ)]$	2.0039	~1.5	~3.1	~7.1	~12.2/6.6 (^{121}Sb/^{123}Sb)	[17]

[a] $[(AP\text{-}ISQ)SbPh_3]^+[BF_4]^-$ is the oxidation product of triphenylantimony(V) 4,6-di-*tert*-butyl-(N-2,6-di-*iso*-propylphenyl)-*o*-amidophenolate with $[Fc]BF_4$.

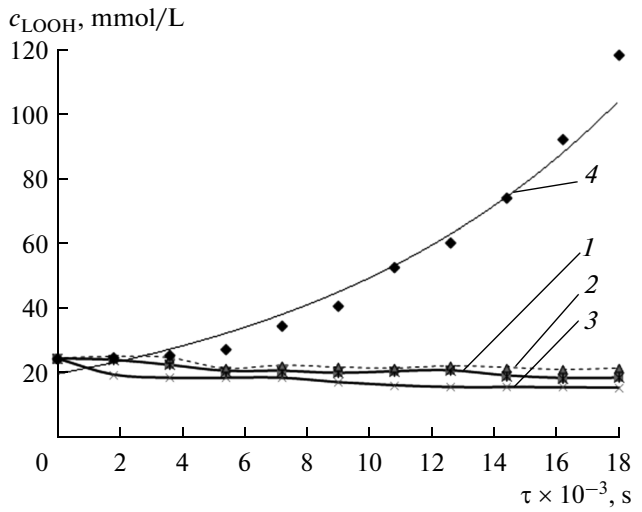

Fig. 7. Kinetic curves of LOOH accumulation in the course of oleic acid oxidation at 60°C in the presence of additives (1 mmol/L): (*1*) (*p*-Tol)$_3$Sb(Cat-NH-Cat), (*2*) Ph$_3$Sb(Cat-NH-Cat), (*3*) (Cyclohex)$_2$Sb(Cat-NH-Cat), and (*4*) control without additives.

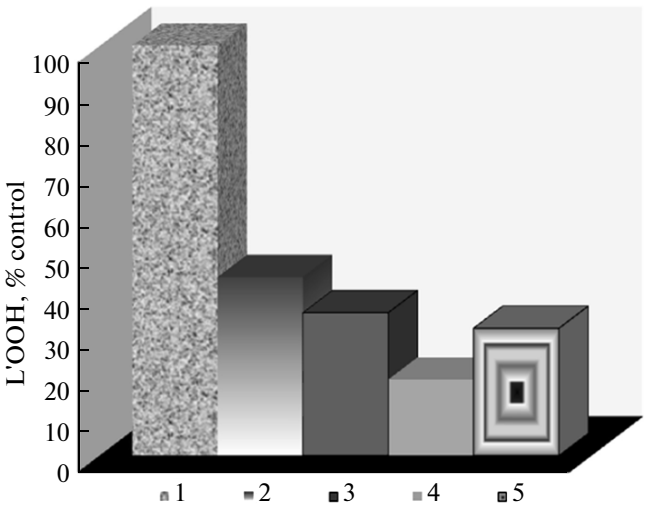

Fig. 8. Relative content of L'OOH in linoleic acid for 144 h of oxidation: (*1*) control without oxidation, (*2*) (*p*-Tol)$_3$Sb(Cat-NH-Cat), (*3*) Et$_2$Sb(Cat-N-Cat), (*4*) (Cyclohex)$_2$Sb(Cat-N-Cat), and (*5*) ionol; T = 30°C, $c_{complex}$ = 1 mmol/L. The content of L'OOH in linoleic acid without additives was accepted to be 100%; (*1*) $c_{L'OOH}$ = 144.0 ± 2.3, (*2*) 63.1 ± 1.2, (*3*) 57.8 ± 1.9, (*4*) 27.5 ± 1.7, and (*5*) 44.9 ± 1.1 nmol/mL.

tion of carbonyl compounds was evaluated in the test with thiobarbituric acid (TBA) from the amount of thiobarbituric acid reactive substances (TBARS).

The influence of the complexes on the change in the hydroperoxide concentration in the course of linoleic acid autooxidation was studied at 30°C for 144 h. In a control experiment, the concentrations of hydroperoxides and TBARS exhibit a regular increase and attain maximum values to the end of the experiment ($c_{L'OOH}$ = 145 mmol/L, c_{TBARS} = 496 nmol/mL). As in the case of oleic acid, the level of hydroperoxide is stabilized in the presence of the studied compounds. After 24 h, the solutions gain a characteristic violet color indicating the formation of the oxidized paramagnetic species. The comparative data on the inhibiting activity of complexes **I**, **IV**, and **V** in the course of linoleic acid autooxidation at 30°C for 144 h are presented in Fig. 8. It is found that the efficiency of the inhibiting effect of complex **IV** is comparable to that of ionol and is twice as large for complex **V**.

The measurement of the TBARS level in 72, 120, and 144 h show that, in the presence of compounds **IV** and **V** and ionol, the parameters are retained lower than those of the control experiment within the whole experiment, indicating the inhibiting activity of the studied compounds (Fig. 9). For complex **I**, the efficiency of the effect decays in time and the TBARS level similar to the control experiment is detected to the end of experiment. The TBARS concentration for compounds **IV** and **V** remains almost unchanged in 120 and 144 h, whereas the activity of ionol decreases. As compared to the control experiment, compound **I** exhibits no increase in the L'OOH concentration (Fig. 9), whereas the TBARS content at the last stage does not differ from that in the control experiment. The levels of TBARS and hydroperoxides do not coincide, which can be explained by the loss of the activity of complex **I** during the decomposition of L'OOH to carbonyl compounds.

The study of the redox processes under the electrochemical experimental conditions shows that the oxidation of hexacoordinate compounds **I**–**III** is reversible and follows the ECE mechanism. As a result, paramagnetic complexes R$_3$Sb(Cat-N-SQ) (**Ia**–**IIIa**) are generated in a solution. The nature of substituents in the aromatic rings at the antimony(V) atom affects the values of redox potentials and stability of these compounds. The electron-donor methyl groups favor the shift of the potentials of complexes **I** and **Ia** to the cathodic region, whereas an opposite effect is detected for compounds **III** and **IIIa** containing the *para*-fluorophenyl groups. The monocationic and monoanionic forms of complexes **Ia** and **II** are most stable, and the oxidation of compound **IIIa** is irreversible. The obtained results indicate the electronic interaction between the redox-active ligand (Cat-NH-Cat, Cat-N-SQ) and aryl groups separated by the antimony(V) atom.

The electrochemical oxidation of pentacoordinate complexes **IV** and **V** proceeds via three consecutive stages. The first and second redox transitions are reversible one-electron processes leading to the formation of mono- and dicationic complexes relatively stable in the time scale of the CV experiment. The electrochemical and chemical oxidation of compounds **IV** and **V** affords [R$'_2$Sb(Cat-N-SQ)]$^+$ detected by UV-Vis, EPR spectroscopy.

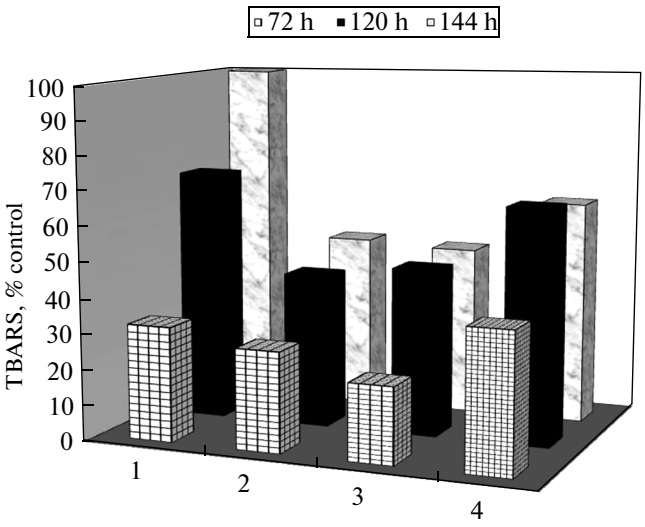

Fig. 9. Change in the relative content of TBARS during linoleic acid autooxidation at 30°C in the presence of the studied compounds (1mmol/L): (*1*) (*p*-Tol)$_3$Sb(Cat-NH-Cat), (*2*) Et$_2$Sb(Cat-N-Cat), (*3*) (Cyclohex)2Sb(Cat-N-Cat), and (*4*) ionol. The content of TBARS in linoleic acid without additives was accepted to be 100%; (*1*) c_{TBARS} = 98.1 ± 4.5, (*2*) 84.9 ± 3.1, (*3*) 65.3 ± 2.7, and (*4*) 98.1 ± 6.7 (in 72 h); (*1*) 291.2 ± 10.8, (*2*) 176.5 ± 9.2, (*3*) 191.8 ± 12.4, and (*4*) 267.9 ± 19.5 (in 120 h); (*1*) 496.2 ± 14.3, (*2*) 241.8 ± 14.7, (*3*) 248.3 ± 11.6, and (*4*) 317.4 ± 15.3 nmol/mL (in 144 h).

The results of electrochemical experiments indicate the activity of complexes **I–V** in the reactions of hydrogen atom abstraction or electron transfer leading to the formation of relatively stable paramagnetic intermediates. A similar reactivity makes it possible to consider these objects as traps of active radicals, i.e., inhibitors of free radical oxidation processes.

The studies show that complexes **I–V** exhibit a pronounced antiradical activity toward the electrogenerated superoxide radical anion, DPPH radical, peroxyl radicals formed by the autooxidation of unsaturated fatty acids, and hydroperoxides. Complexes **I**, **IV**, and **V** are most active. Complexes **IV** and **V** are involved in the decomposition of hydroperoxides to molecular products (carbonyl compounds) and exert a prolonged effect in the course of linoleic acid autooxidation with the retention of the inhibiting effect for a long time. The efficiency of the effects of compounds **I–V** is comparable, and some complexes exhibit the results obtained for the standard phenol antioxidant (2,6-di-*tert*-butyl-4-methylphenol).

The antiradical activity of complexes **I–V** is mainly due to the tridentate O,N,O-donor ligand capable of existing in several redox states. The coordination of the oxidized form of the ligand to the antimony(V) atom increases the stability of the paramagnetic species formed in reactions of electron transfer and hydrogen atom abstraction. Due to the electronic interaction between the redox-active ligand and hydrocarbon groups at the antimony atom, their nature exerts an effect on the redox properties and antiradical activity of complexes **I–V**.

ACKNOWLEDGMENTS

This work was supported by the President of the Russian Federation (grant MK-445.2014.3), the Presidium of the Russian Academy of Sciences (program no. 8), and the Russian Foundation for Basic Research (project nos. 12-03-00513 and 14-03-00578).

REFERENCES

1. Cador, O., Chabre, F., Dei, A., et al., *Inorg. Chem.*, 2003, vol. 42, p. 6432.
2. Chaudhuri, P., Hess, M., Hildenbrand, K., et al., *Inorg. Chem.,* 1999, vol. 38, p. 2781.
3. Bruni, S., Caneschi, A., Cariati, F., et al., *J. Am. Chem. Soc.,* 1994, vol. 116, p. 1388.
4. Dei, A., Gatteschi, D., Sangregrio, C., and Sorace, L., *Acc. Chem. Res.*, 2004, vol. 37, no. 11, p. 827.
5. Chaudhuri, P., Hess, M., and Wieghardt, K., *Angew. Chem., Int. Ed. Engl.*, 1999, vol. 38, p. 1095.
6. Zarkesh, R.A., Ziller, J.W., and Heyduk, A.F., *Angew. Chem., Int. Ed. Engl.*, 2008, vol. 47, p. 4715.
7. Wright, D.D. and Bromn, S.N., *Inorg. Chem.*, 2013, vol. 52, no. 14, p. 7831.
8. Shekar, S. and Brown, S.N., *Organometallics*, 2013, vol. 32, no. 2, p. 556.
9. Lu, F., Zarkesh, R.A., and Hyeduk, A.F., *Eur. J. Inorg. Chem.*, 2012, p. 467.
10. Girgis, A.I. and Balch, A.L., *Inorg. Chem.*, 1975, vol. 14, p. 2724.
11. Stegmann, H.B. and Srheffler, K., *Chem. Ber.*, 1970, vol. 103, p. 1279.
12. Larsen, S.K. and Pierpont, C.G., *J. Am. Chem. Soc.*, 1988, vol. 110, p. 1827.
13. Camacho-Camacho, C., Tlahuext, H., North, H., and Contreras, R., *Heteroatom Chem.*, 1998, vol. 9, p. 321.
14. Szigethy, G. and Heyduk, A.F., *Dalton Trans.*, 2012, vol. 41, p. 8144.
15. Szigethy, G., Shaffer, D.W., and Heyduk, A.F., *Inorg. Chem.*, 2012, vol. 51, p. 12606.
16. Munh, R.F., Zarkesh, R.A., and Heyduk, A.F., *Dalton Trans.*, 2013, vol. 42, p. 3751.
17. Poddel'sky, A.I., Somov, N.N., Kurskii, Yu.A., et al., *J. Organomet. Chem.*, 2008, vol. 693, p. 3451.
18. Poddel'sky, A.I., Vavilina, N.N., Somov, N.N., et al., *J. Organomet. Chem.*, 2009, vol. 694, p. 3462.
19. Abakumov, G.A., Poddel'sky, A.I., Grunova, E.V., et al., *Angew. Chem. Int. Ed.*, 2005, vol. 44, p. 2767.
20. Cherkasov, V.K., Abakumov, G.A., Grunova, E.V., et al., *Chem.-Eur. J.*, 2006, vol. 12, p. 3916.
21. Poddel'sky, A.I., Smolyaninov, I.V., Somov, N.V., et al., *J. Organomet. Chem.*, 2010, vol. 695, p. 530.
22. Ilyakina, E.V., Poddel'sky, A.I., Cherkasov, V.K., and Abakumov, G.A., *Mendeleev Commun.*, 2012, vol. 22, p. 208.

23. Smolyaninov, I.V., Okhlobystin, A.O., Poddel'sky, A.I., et al., *Dokl. Chem.*, 2009, vol. 427, no. 1, p. 147.
24. Smolyaninov, I.V., Okhlobystin, A.O., Poddel'sky, A.I., et al., *Russ. J. Coord. Chem.*, 2011, vol. 36, no. 1, p. 12.
25. Arsenyev, M.V., Shurygina, M.P., Poddel'sky, A.I., et al., *J. Polymer Research*, 2013, vol. 20, p. 98.
26. Oliveira, L.G., Silva, M.M., Paula, F.C.S., et al., *Molecules*, 2011, vol. 16, p. 10314.
27. Rocha, M.N., Nogueira, P.M., and Demicheli, C., *Bioinorg. Chem. Appl.*, 2013.
28. Asghar, F., Badshan, A., Shah, A., et al., *J. Organometal. Chem.*, 2012, vol. 717, p. 1.
29. Smolyaninov, I.V., Antonova, N.A., Poddel'sky, A.I., et al., *J. Organomet. Chem.*, 2011, vol. 696, p. 2611.
30. Smolyaninov, I.V., Poddel'sky, A.I., Antonova, N.A., et al., *Russ. J. Coord. Chem.*, 2013, vol. 39. no. 2, p. 165.
31. Smolyaninov, I.V., Antonova, N.A., Poddel'sky, A.I., et al., *Appl. Organomet. Chem.*, 2012, vol. 26, p. 277.
32. Smolyaninova, S.A., Poddel'sky, A.I., Smolyaninov, I.V., et al., *Russ. J. Gen. Chem.*, 2013, vol. 83, no. 10, p. 1900.
33. Smolyaninov, I.V., Antonova, N.A., Poddel'skii, A.I., et al., *Dokl. Chem.*, 2012, vol. 443, no. 1, p. 72.
34. Gordon, A. and Ford, R., *The Chemist's Companion: A Handbook of Practical Data, Techniques, and References*, New York: Wiley, 1972.
35. Tyurin, V.Yu., Meleshonkova, N.N., Dolganov, A.V., et al., *Izv. Akad. Nauk, Ser. Khim.*, 2011, no. 4, p. 633.
36. Vladimirov, Yu.A. and Archakov, A.I., *Perekisnoe okislenie lipidov v biologicheskikh membranakh* (Peroxidation of Lipids in Biological Membranes), Moscow: Nauka, 1972.
37. Dieffenbacher, A. and Pocklington, W.D., *Standard Methods for the Analysis of Oils, Fats and Derivatives*, Oxford: Blockwell Scientific Publ. Ltd., 1992.
38. Piskunov, A.V., Sukhoshkina, O.Yu., and Smolyaninov, I.V., *Russ. J. Gen. Chem.*, 2010, vol. 80, no. 4, p. 790.
39. Smolyaninov, I.V., Poddel'sky, A.I., and Berberova, N.T., *Russ. J. Electrochemistry*, 2011, vol. 47, no. 11, p. 1295.
40. Ren, T., *Inorg. Chim. Acta*, 1995, vol. 22, nos. 1–2, p. 195.
41. Korotkova, E.I., Karbainov, Y.A., and Shevchuk, A.V., *J. Electroanal. Chem.*, 2002, vol. 518, p. 56.
42. Korotkova, E.I., Mamaeva, E.A., Bashkatova, N.V., et al., *Khim.-Farm. Zh.*, 2004, vol. 38, no. 3, p. 52.
43. Ziyatdinova, G.K., Gil'metdinova, D.M., and Budnikov, G.K., *Zh. Anal. Khim.*, 2005, vol. 60, no. 1, p. 56.
44. Korotkova, E.I., Lipskikh, O.I., Kiseleva, M.A., et al., *Khim.-Farm. Zh.*, 2008, vol. 42, no. 8, p. 45.
45. Dorozhko, E.V. and Korotkova, E.I., *Khim.-Farm. Zh.*, 2011, vol. 44, no. 10, p. 53.
46. Denisov, E.T. and Denisova, T.G., *Oxidation and Antioxidants in Organic Chemistry and Biology*, Boca Raton; New York: CRC Press, 2005, p. 1024.
47. Sawier, D.T. and Seo, E.T., *Inorg. Chem.*, 1977, vol. 16, p. 499.
48. Sawier, D.T., Gibian, M.J., Morrison, M.M., and Seo, E.T., *Inorg. Chem.*, 1978, vol. 18, p. 627.
49. Chin, D.H., Chiericato, G., Nanni, E.J., and Sawyer, D.T., *J. Am. Chem. Soc.*, 1982, vol. 104, no. 5, p. 1296.
50. Nanni, E.J., Stallings, M.D., and Sawier, D.T., *J. Am. Chem. Soc.*, 1980, vol. 102, p. 4481.
51. Blois, M.S., *Nature*, 1958, vol. 181, p. 1199.
52. Nakanishi, I., Miyazaki, K., Shimada, T., et al., *Org. Biomol. Chem.*, 2005, vol. 3, p. 626.
53. Bondet, V., Brand-Williams, W., and Berset, C., *Lebensm.-Wiss. Technol.*, 1997, vol. 30, p. 609.
54. Baciocchi, E., Calcagni, A., and Lanzalinga, O., *Org. Chem.*, 2008, vol. 73, p. 4110.
55. Tyurin, V.Yu., Dzhingvei, Zh., Moiseeva, A.A., et al., *Dokl. Ross. Akad. Nauk*, 2013, vol. 450, no. 5, p. 543.
56. Smolyaninov, I.V., Poddel'sky, A.I., Berberova, N.T., et al., *Russ. J. Coord. Chem.*, 2010, vol. 36, no. 9, p. 644.
57. Stegmann, H.B. and Srheffler, K., *Angew. Chem., Int. Ed. Engl.*, 1970, vol. 9, p. 456.
58. Stegmann, H.B. and Srheffler, K., *Angew. Chem., Int. Ed. Engl.*, 1971, vol. 10, p. 499.

Translated by E. Yablonskaya